

Oscillatory Magma Crystallization by Feedback between the Concentrations of the Reactant Species and Mineral Growth Rates

by YIFENG WANG AND ENRIQUE MERINO

Department of Geological Sciences, Indiana University, Bloomington, Indiana 47405

(Received 21 December 1991; revised typescript accepted 10 August 1992)

ABSTRACT

During crystallization of silicate magmas, silica polymers advect into the reaction zone carrying other chemical species with them. If some species forming minerals are more abundant relative to Si in the liquid than in the minerals, then the species become more concentrated in the reaction zone as crystallization progresses. This enrichment may cause mineral growth rates to increase, thereby accelerating the advection of silica and further increasing the concentrations. This positive feedback may be slowed down by the depletion of other reactant species that have lower concentration ratios to Si in the liquid than in the minerals. A quantitative transport-reaction model that incorporates these competing effects, mass-action mineral-growth rate laws, and diffusion plus advection, shows that the feedback can cause oscillatory crystallization. The model represents a plausible mechanism for the origin of repetitive igneous layering. It predicts the repeated layering itself, its occasional occurrence in general, its common occurrence in alkaline rocks, and paired layering. Also, it accounts directly for a significant property of microrhythmic layering: that the oscillatory modes of two or more minerals are spatially staggered.

INTRODUCTION

Repetitive layering in igneous rocks commonly consists of spatial modal alternations of light and dark layers (e.g., Emeleus, 1963; Jahns & Tuttle, 1963; Leveson, 1963, 1966; Sørensen, 1969; Griffin *et al.*, 1974; McBirney & Noyes, 1979; Elliston, 1984; Parsons, 1987; Naslund *et al.*, 1991). The light layers commonly consist of plagioclase or alkali feldspar. The dark ones may consist of biotite, amphibole, pyroxene, and olivine, and, in at least one instance, dark cloudy quartz (McBirney *et al.*, 1990). Spacing of the layers ranges from 0.1 cm to 10 cm or more. The repeated layers occur in various rock types, from felsic to mafic, and they may be orbicular (Fig. 1A,B), planar (e.g., Boudreau, 1987), cylindrical (Parsons, 1987, p. 421), or scalloped (McBirney & Noyes, 1979, plate 5C). Also, one set of alternating layers can cut across another (McBirney & Noyes, 1979, plate 4A).

Ideas about the origin of repetitive layering in igneous rocks fall into four groups:

(1) Some layering has been attributed to crystal settling (e.g., Wager & Brown, 1968; Irvine, 1987a), but considerable evidence has been cited against this idea for some specific cases (Campbell, 1978; McBirney & Noyes, 1979).

(2) The layering is produced by thermal oscillations during magma cooling; these oscillations can be caused by interaction among latent heat release, heat conduction, and crystallization rate (Brandeis *et al.*, 1984), or by an (assumed) delayed response of crystallization rate to temperature change (Samoylovich, 1979; Allègre *et al.*, 1981).

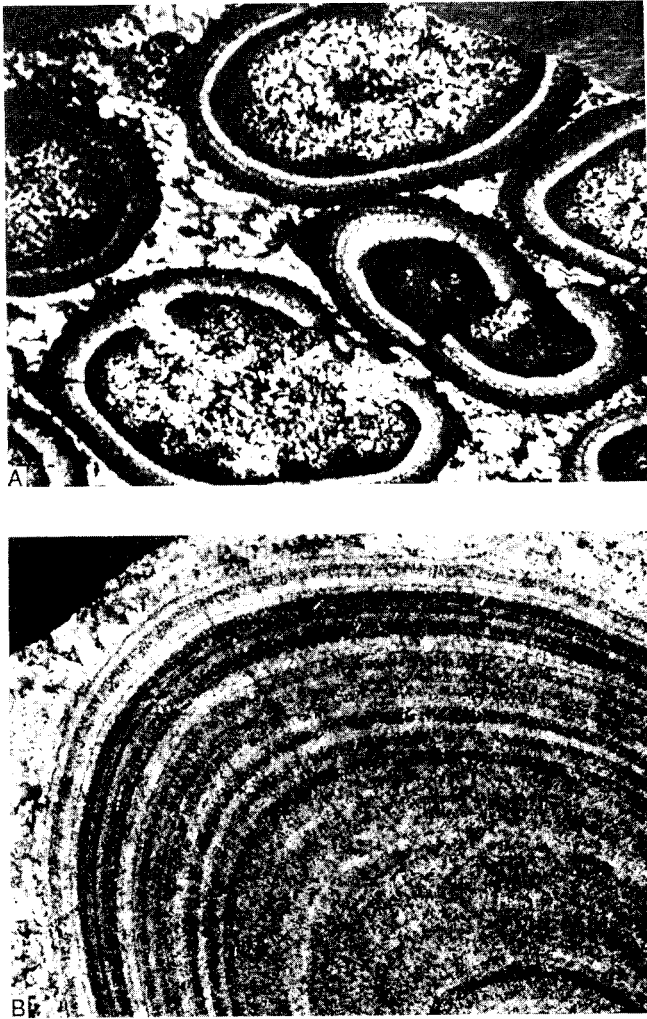


FIG. 1. (A) Orbicule (12 cm across) in diorite from Corsica, showing hornblende-rich layers that have one side sharp and the other diffuse; the light mineral is plagioclase. (Photograph by B. Fritz, Strasbourg.) (B) Orbicule (20 cm across) in diorite from Epoo, Finland, consisting of layers alternatively richer in biotite and plagioclase. The minimum size of the biotite crystals in the biotite-poor layers is 0.05 mm, and the average size is only slightly larger. Plagioclase crystals are 5–10 times larger.

(3) Repetitive layering in igneous rocks results from temperature-controlled periodic nucleation (McBirney & Noyes, 1979; Maaløe, 1987).

Mechanisms (2) and (3) fail to account for the fact that the repeated layers are not always parallel to a cooling front, notably in the case of concentric layering in orbicules. And, in any case, the repetitive layering in orbicules, given their small size, is certain to be spatially uniform in temperature, because heat diffusivity in rocks (10^{-2} cm²/s, Verhoogen *et al.*, 1970, p. 645) is many orders of magnitude greater than chemical diffusivity (10^{-8} cm²/s or less, Chekhmir & Epel'baum, 1991, fig. 11).

(4) Repetitive layering has been attributed also to Ostwald ripening (Boudreau, 1987; McBirney *et al.*, 1990), a mechanism based on the dependence of free energy on crystal size.

Two observations can be made on this mechanism. (A) Typically [see experiments by Nabelek *et al.* (1978, figs. 2 and 3) and especially by Baronnet (1982), whose fig. 11 is reproduced as fig. 9 by Morse & Casey (1988); and see Berner (1980, p. 94)], this dependence applies only to crystal sizes far less than the size of the smallest crystals found in layered rocks (such as those in Fig. 1B). (B) Ostwald ripening implies that increases in the local mode of a mineral should be produced by increases in crystal size. Thus, in cases such as that described by McBirney & Noyes (fig. 11, 1979), where it was shown that an increase in plagioclase mode exactly corresponds to the smallest crystal size, it may be inferred that Ostwald ripening did not effect the layering.

Finally, the last three mechanisms surveyed above consider only one mineral and ignore chemical interactions (through species in common) among two or more minerals crystallizing together. It is probably these chemical interactions among minerals that intrinsically produce the out-of-phase modal variations characteristic of rhythmic layerings.

Here we propose a new mechanism to produce repetitive layers in igneous rocks. It involves feedbacks between nonlinear mineral-growth rates and segregation of chemical components at crystallization fronts, and does not have the drawbacks pointed out above. We first discuss these feedbacks qualitatively, then give a quantitative model incorporating them, and finally discuss some of its implications. Symbols used in the equations are listed in Table 1.

FEEDBACK AND OSCILLATORY MECHANISM

Let us consider the model system sketched in Fig. 2. Its main feature is a reaction zone, $0 < X < L_r$, within which crystals and melt coexist, and outside of which there is only melt on one side and only crystals on the other. Nucleation and crystal growth take place only within the reaction zone. Concentration profiles of chemical species remain roughly flat across the reaction zone. As shown in Fig. 2, we place the origin of coordinates at the left side of the moving reaction zone.

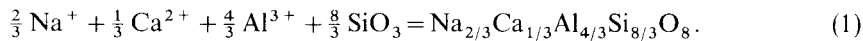
The volume of a silicate melt can be regarded as consisting primarily of silica polymers (or of their oxygens), the silicon ion being a network-builder (e.g., Hess, 1989, p. 59ff). All other species, the modifiers, can be regarded as 'riding' on that framework of supporting polymers. Both because the melt volume consists mainly of silica polymers, and because the volume added by the network-modifiers tends to be compensated for by the structural collapse they produce, the concentration of silicon in the melt, in moles Si/cm³ of melt, should be roughly constant. The polymer framework thus plays a dual role in mass transfer in magmas: it is the supporting medium through which other species diffuse, and it can transport these other species by advection—much as water transports solutes in low-temperature aqueous solutions.

Upon mineral growth, the reaction zone advances into the melt, bringing about advection of the silica-polymer framework into the reaction zone (Fig. 2). The framework carries with it both modifier ions and the other network-builders (which occur only in minor amounts), such as Fe³⁺ and some Al³⁺. If the minerals produced in the reaction zone have density greater than that of melt, there will be a tendency for a gap to open up between the reaction zone and the melt—a gap that is, of course, automatically and continuously closed by an additional advection driven by mechanical pressure. A species entering a growing mineral, and being (relative to Si) more concentrated in the melt than in the mineral, must accumulate in the reaction zone. The accumulation may in turn cause mineral-growth rates to increase, which causes further accumulation, and so on. This positive feedback can bring about oscillatory crystallization; this is shown below quantitatively.

TABLE I
Symbols

A_j	chemical species j in the melt
a_{ij}	exponent on the j th species concentration in rate law of the i th mineral reaction, equation (3)
C	concentration vector, $[c_1, c_2, \dots, c_q]^T$, equation (5)
C^0	concentration vector C in the reaction zone
C^L	concentration vector C at $X=L$
\bar{C}^0	C^0 at a steady state
c_j	concentration of species j in melt (mol/cm ³ of melt)
c_j^L	concentration of species j outside the boundary layer
c_s	Si concentration (mol/cm ³ of melt)
D	diagonal diffusion coefficient matrix, equation (5)
D_j	diffusivity of species j in melt
H	matrix (obtained by linear instability analysis) characterizing the behavior of equation (10) near a steady state, equation (12)
J	matrix of derivatives of reaction rates with respect to concentrations, $[\partial r_i / \partial c_j]_{p \times q}$, or Jacobian, evaluated at the steady state, equation (12)
k_i	rate constant of reaction i , equation (3)
L	distance from left side of reaction zone at which concentrations first become constant, Fig. 2
L_r	thickness of the reaction zone, Fig. 2
M	stoichiometric vector for Si, $[m_1, m_2, \dots, m_p]^T$
m_i	moles of Si involved in reaction i , equation (4)
N	stoichiometric matrix, $[n_{ij}]_{p \times q}$, equation (2)
n_{ij}	stoichiometric coefficient of species j other than Si in reaction i , equation (2)
p	number of minerals (and mineral reactions) involved
q	number of chemical species A_j (other than silica) involved
R	reaction rate vector, $[r_1, r_2, \dots, r_p]^T$
r_i	rate of reaction i (mol/cm ³ s), equation (3)
T	typical time for a pair of layers to form, equation (16)
t	time
V_{pl}	molar volume of plagioclase
V_{bi}	molar volume of biotite
X	distance from left side of reaction zone
β	ratio of reaction-zone to boundary-layer thicknesses
γ_j	dimensionless concentration of species j at $X=L$ (see Appendix)
η	$\theta_{Ca^{2+}}$, times a function of dimensionless concentrations (see Appendix)
θ_j	diffusivity ratio of Al ³⁺ to species j (see Appendix)
λ_i	dimensionless rate constant of reaction i (see Appendix)
δC^0	small perturbation of C^0 from its steady-state value, equation (11)
ϕ	volume fraction of liquid in reaction zone
ω	advection velocity of silica framework toward reaction zone

To illustrate this oscillatory mechanism, we consider the hypothetical case in which plagioclase of fixed An₃₃ composition crystallizes from a silicate melt, according to the overall reaction



(For simplicity and because it is not known how growth kinetics and solid-solution composition modify each other, we here take a fixed composition for plagioclase during the crystallization. This simplification does not affect the essence of the dynamics of the feedback we propose.) If the Ca/Si and Al/Si molar ratios in the melt are respectively $> 1/8$ and $< 1/2$, the growth of this plagioclase must produce accumulation of Ca²⁺ and depletion of Al³⁺ in the reaction zone. By analogy with mass-action rate laws routinely used for aqueous–mineral reactions, we assume now that the rate of reaction (1) is proportional to $(c_{\text{Ca}^{2+}}^0)^a (c_{\text{Al}^{3+}}^0)^b$, where c_i^0 is the concentration of subscripted species (moles i /cm³ of melt) in the reaction zone, and a and b are positive. Na⁺ does not enter this rate law because it is assumed to diffuse

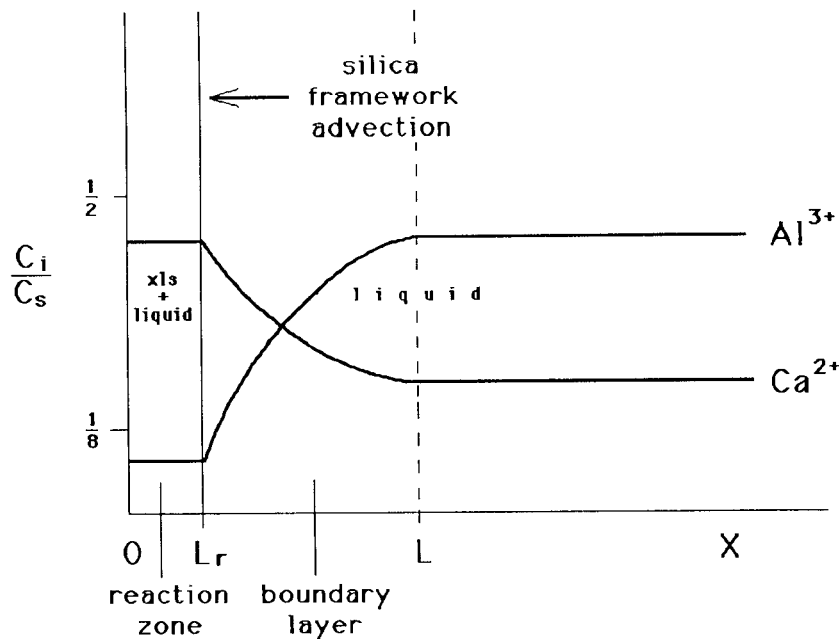


FIG. 2. Model system for the crystallization of minerals from a liquid. The origin is placed at the left side of the reaction zone, within which crystals (xls) coexist with liquid. Outside the reaction zone there is only melt on the right and only crystals on the left. Nucleation and crystal growth take place only within the reaction zone, and concentration profiles of chemical species remain roughly flat across it. Silicate polymers advect toward the reaction zone, carrying other ions. The boundary layer is defined by the distance at which species' concentrations first become approximately constant. Shown are typical profiles of Ca^{2+} and Al^{3+} concentrations (relative to that of Si^{4+}) in the liquid during crystallization of An_{33} plagioclase. For An_{33} plagioclase crystallization, because the far-away concentrations of Ca^{2+} and Al^{3+} , relative to Si^{4+} , are by assumption $> 1/8$ and $< 1/2$, respectively, Ca^{2+} starts to accumulate in the reaction zone and Al^{3+} starts to become depleted. Feedback is then triggered, and it produces the concentration and mode oscillations shown in Fig. 4.

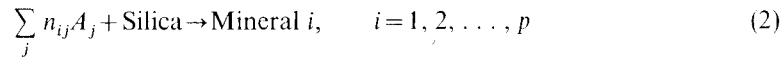
much faster than other ions relative to the growth rate [the same would apply to K^+ if it were present, as its diffusivity is also high (fig. 11 in Chekhmir & Epel'baum, 1991)], and Si does not enter the law either because its concentration can be regarded as constant, as discussed above. If a is large enough, the accumulation of Ca^{2+} should accelerate the growth of plagioclase An_{33} . Advection of silica polymers into the reaction zone thus must accelerate too, carrying more Ca^{2+} ions to the reaction zone, again accelerating Ca^{2+} accumulation and plagioclase growth, and further depleting Al^{3+} . Eventually, the local Al^{3+} concentration becomes so low that the growth rate decreases. Now the accumulated Ca^{2+} diffuses away from the reaction zone back into the melt, so growth becomes even slower. However, Al^{3+} concentration in the reaction zone then recovers, and another cycle of oscillation begins.

The feedback described is still more likely to occur where two or more minerals, rather than just one, grow simultaneously, because now several species may accumulate at the front. For instance, for the plagioclase-biotite repetitive layering shown in Fig. 1B, all of Ca^{2+} , Mg^{2+} , and Fe^{2+} may accumulate in the reaction zone, and their accumulation accelerates plagioclase and biotite growth. This should require the silicate network to advect faster into the reaction zone; and this faster supply would further speed up the accumulation of the three species. In addition, this positive feedback should be strengthened by the increase in Mg^{2+} and Fe^{2+} concentrations produced by plagioclase growth, which does not consume these ions, and by the concomitant increase in Ca^{2+} concentration produced by biotite growth,

which does not consume Ca^{2+} . In addition, the two minerals compete for Al^{3+} . These mineral–mineral chemical feedbacks tend to stagger oscillations in the growth of the two minerals and to make them occur out of phase, as is routinely observed. The mechanism proposed is self-organizational (Nicolis & Prigogine, 1977), and is very similar to the mechanism responsible for textural alternations of quartz fibers in agates from flood basalts (Wang & Merino, 1990).

QUANTITATIVE MODEL OF OSCILLATORY CRYSTALLIZATION

We assume that p minerals crystallize in the reaction zone (Fig. 2), according to the following reactions:



where A_j ($j = 1, 2, \dots, q$) is one of the species in the melt such as Na^+ , K^+ , Ca^{2+} , Al^{3+} , Mg^{2+} , Fe^{2+} , OH^- (but not silica), and n_{ij} is the stoichiometric coefficient of A_j in reaction i . We write the rate of reaction i , r_i , as

$$r_i = k_i \prod_j (c_j^0)^{a_{ij}} \quad (3)$$

where c_j^0 is the concentration of species j in the reaction zone, k_i (a function of temperature) is the rate constant of reaction i , and $a_{ij} \geq 0$.

Work on the kinetics of melt crystallization has focused on the dependence of growth rates on temperature (e.g., Kirkpatrick, 1976; Ghiorso, 1987). However, growth rate laws of this type [e.g., Ghiorso, 1987, equation (3)] are not applicable to the feedback we propose here, because for conditions far from chemical equilibrium—such as we explore—the law comes to depend only on temperature and not on melt composition (Ghiorso, 1987, p. 293), and the mass-action effects that are crucial in our mechanism disappear. Therefore, by analogy with mass-action kinetic laws used in low-temperature geochemistry, we assume in equation (3) that the reaction rate is proportional to the reactant concentrations, raised to positive exponents. As explained above, silicon concentration in the melt does not appear in equation (3). (A refinement of the model would use rate laws explicitly containing concentrations of silica or different silicate polymers.) It should be noted that, because the nucleation rate is proportional to the concentrations of species, nucleation is implicitly included in equation (3).

Advection velocity, ω , of the silica framework relative to the reaction zone is then expressed as

$$\omega = \sum_i m_i r_i L_r / c_s \quad (4)$$

where m_i ($i = 1, 2, \dots, p$) is the stoichiometric coefficient of Si in reaction i ; and c_s , the concentration of Si (mol Si/cm³ liquid), is assumed to be constant (see above). We now write continuity equations for all relevant species in the system shown in Fig. 2:

For $0 < X < L_r$:

$$\phi L_r \frac{dC^0}{dt} = D \left. \frac{\partial C}{\partial X} \right|_{X=L_r^+} + L_r \left(\frac{C^0}{C_s} M^T - N^T \right) R \quad (5)$$

For $L_r < X < L$:

$$\frac{\partial C}{\partial t} = D \frac{\partial^2 C}{\partial X^2} + \omega \frac{\partial C}{\partial X} \tag{6}$$

and, at $X=L$,

$$C = C^L \tag{7}$$

where $C = [c_1, c_2, \dots, c_q]^T$ and c_j is the concentration of species j (mol/cm³) outside the reaction zone; $D = \text{diagonal } [D_1, D_2, \dots, D_q]$ and D_j is the diffusion coefficient of species j ; $N = [n_{ij}]_{p \times q}$; $R = [r_1, r_2, \dots, r_p]^T$ is the vector of reaction rates for the p reactions; q is the number of species; ϕ is the volume fraction of liquid in the reaction zone; t is time; X is the distance from the left side of the reaction zone; and L is the distance at which C first becomes a constant C^L (Fig. 2).

Integrating equation (6) over the boundary layer ($L_r < X < L$) and using the approximations

$$\int_{L_r}^L C \, dX \approx \frac{(L - L_r)(C^0 - C^L)}{2} \tag{8}$$

$$\left. \frac{\partial C}{\partial X} \right|_{X=L} \approx \frac{C^L - C^0}{L - L_r} \tag{9}$$

equations (5)-(7) are reduced to

$$(1 + \beta\phi) \frac{dC^0}{dt} = \frac{2D}{(L - L_r)^2} (C^L - C^0) + 2\beta \left(\frac{C^L M^T}{c_s} - N^T \right) R \tag{10}$$

where C^0 is C in the reaction zone and $M = [m_1, m_2, \dots, m_p]^T$. Equation (10) governs the temporal evolution of the species concentrations, C^0 , in the reaction zone; β is the ratio $L_r/(L - L_r)$. The first term on the right of equation (10) represents the diffusion flux entering the reaction zone; the second term represents the advection flux into the reaction zone minus the mass consumption by the chemical reactions within it.

To see if C^0 can be oscillatory with time, we carry out a linear instability analysis (Cook, 1986, pp. 14-46; see also Wang & Merino, 1992, appendix) of equation (10) around its steady-state solutions, which are designated by \bar{C}^0 and are obtained from equation (10) by setting $dC^0/dt = 0$. Introducing a small perturbation δC^0 of C^0 from \bar{C}^0 , inserting $\delta C^0 + \bar{C}^0$ into equation (10), and dropping nonlinear terms in δC^0 , we obtain

$$\frac{d \delta C^0}{dt} = H \delta C^0 \tag{11}$$

where

$$H = \frac{2}{1 + \beta\phi} \left[-\frac{D}{(L - L_r)^2} + \beta \left(\frac{C^L M^T}{c_s} - N^T \right) J \right] \tag{12}$$

where $J = [\partial r_i / \partial c_j]_{p \times q}$ evaluated at the steady state, and $\partial r_i / \partial c_j \geq 0$ for all minerals (i) and species in the liquid (j). J characterizes how strongly mineral growth rates depend on species concentrations in the liquid, near the steady state. The behavior of equation (10) near the steady state is determined by matrix H : if one or more eigenvalues of H are positive, the perturbation, δC^0 , grows with time; the system is then unstable at the steady state and tends to move away from it, and equation (10) may then have oscillatory solutions. The first term inside the brackets in equation (12) makes a negative contribution to the eigenvalues and

therefore tends to make the system stable. The second term represents the effects of segregation, $C^L M^T / c_s - N^T$, and mineral-growth kinetics, J , and tends to make the system unstable to oscillations if some components of matrix $C^L M^T / c_s - N^T$ are sufficiently positive, i.e., if some reactant species are segregated. It should be noted that the diffusivities enter not only the first term (explicitly) but also the second term (implicitly), through J .

From the above linear instability analysis, the behaviors of equation (10) can be described by phase diagrams. Figure 3 is one such phase diagram for a system in which plagioclase An_{33} crystallizes, with Ca^{2+} accumulated and Al^{3+} depleted in the reaction zone. With the parameter values indicated in the caption to Fig. 3, equation (10) can have oscillatory solutions if

$$D_{Al^{3+}} / D_{Ca^{2+}} < 0.1 \quad (13)$$

and

$$\frac{(8 - c_s / c_{Ca^{2+}}^L)}{(8 - 4c_s / c_{Al^{3+}}^L)} < -30. \quad (14)$$

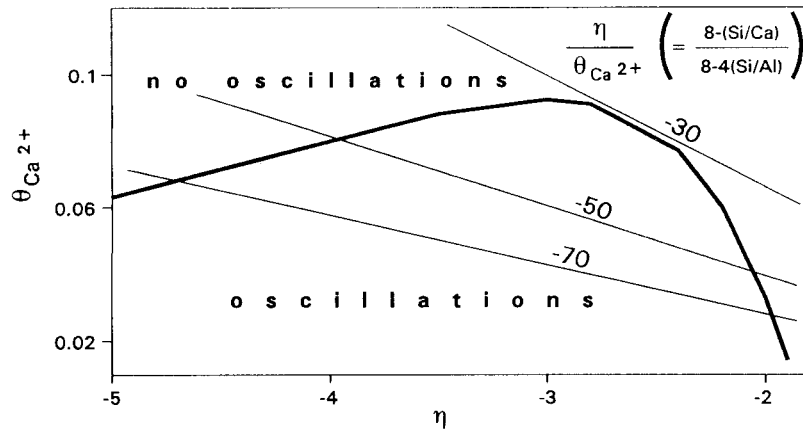
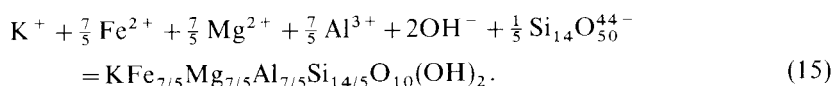


FIG. 3. Behavior diagram for the growth of An_{33} plagioclase only. The parameter $\theta_{Ca^{2+}}$ along the vertical axis is equal to the Al^{3+} diffusivity to Ca^{2+} diffusivity ratio. The parameter η along the horizontal axis is a function of melt composition and ion diffusivities (see definitions of $\theta_{Ca^{2+}}$ and η in Appendix). The inclined straight lines are contours of $\eta / \theta_{Ca^{2+}}$, which is a function (shown in parentheses) of melt composition only; the specific form of this function depends on mineral stoichiometry. The crystallization is oscillatory (as shown in Fig. 4) below the curve, and non-oscillatory above. The curve is obtained by linear instability analysis (text), using the plagioclase rate law, $r_{pl} = k_{pl}(Ca^{2+})^2(Al^{3+})$ and $[(8/3)\gamma_{Al^{3+}} - (4/3)]\lambda_{pl} = 0.3$ (see the definitions of $\gamma_{Al^{3+}}$ and λ_{ab} in the Appendix). Oscillations thus require $\eta / \theta_{Ca^{2+}}$ to be < -30 , which requires Al/Si to be close to, but less than, $1/2$ (as shown in Fig. 2).

Condition (13)—which implies that, for the crystallization of melt to be oscillatory, the accumulated liquid species must have a higher diffusivity than does the depleted species—is readily satisfied in actual systems because, indeed, monovalent cations have greater diffusivities than bivalent ones, which have greater diffusivities still than trivalent ones (fig. 11 in Chekhmir & Epel'baum, 1991). The requirement that the accumulated species must have higher diffusivity also applies to two-mineral systems, as we have confirmed by numerical simulations of equation (10) not reported here. For any value of $c_{Ca^{2+}}^L / c_s > 1/8$, condition (14) for oscillation requires that $c_{Al^{3+}}^L / c_s$ be very close to, but less than, $1/2$. This restrictive condition is obtained here for the particular case of plagioclase crystallizing from a

silicate liquid with the assumed growth rate law given in the caption to Fig. 3, but it suggests that the proposed mechanism should work only occasionally, i.e., for very narrow compositional ranges. This would explain why igneous repetitive layering of the self-organizational kind is not ubiquitous. For cases where two or more minerals crystallize together, the range of $c_{\text{Al}^{3+}}^L/c_s$ for which oscillations are allowed is wider but still restricted. The linear instability analysis also shows that, for the plagioclase to crystallize oscillatorily, the exponent on Ca^{2+} concentration in the rate law should be larger than unity.

Equation (10) has been solved numerically for the growth of two minerals (plagioclase and biotite), with the choice of parameter values guided by the linear instability analysis for the plagioclase-only case. Plagioclase is assumed to form through reaction (1), and biotite through



The numerical solutions show that the proposed feedback can produce oscillatory crystallization for any set of minerals. One set of numerical solutions for plagioclase-biotite layering is shown in Fig. 4. In Fig. 4B the layer spacing equals about 15 boundary layers, $15(L-L_r)$. This predicted banding scale is consistent with observations if $(L-L_r)$ were between 0.01 and several centimeters, a range that seems reasonable to us but that we cannot check independently. (For other mineral pairs and other parameter values, the spacing predicted would be different, but not by an order of magnitude.) The time to form each pair of plagioclase and biotite layers is predicted by

$$T \approx \frac{(L-L_r)^2}{2D_{\text{Al}^{3+}}} \quad (16)$$

or from half to several years if Al^{3+} diffusivity in silicate melts is of order $10^{-9} \text{ cm}^2/\text{s}$ (Hess, 1989, table 5.2; and fig. 11 in Chekhmir & Epel'baum, 1991). Equation (16) is obtained by scaling equation (10) for the case of Al^{3+} : we divide equation (10) by $2D_{\text{Al}^{3+}}/(L-L_r)^2$, and then define the time scaling factor such that the coefficient on the left side is unity. The factor $1 + \beta\phi$ is approximately equal to one.

By using different values for exponents in the reaction rate laws and different starting liquid composition, we obtain numerical solutions that simulate paired layers of plagioclase and biotite (Fig. 5); the proposed model can thus produce doublets of the type observed in the Stillwater Complex (fig. 1 in Boudreau, 1987) and elsewhere.

DISCUSSION AND CONCLUSIONS

The feedback we propose here to account for oscillatory crystallization of minerals from melt is simple. Crystallization of minerals from a silicate liquid implies the advance of a crystallization front into the liquid—or conversely, the advection of silica polymers, and the species attached to them, into the reaction zone, if the latter is adopted as origin of coordinates. Growth of mineral grains in this zone causes certain mineral-forming species, those with high concentration relative to Si, to accumulate in it. If the mineral growth rates (of the mass-action type adopted here) depend strongly enough on the concentration of those species, then their accumulation accelerates mineral growth. Faster mineral growth in turn enhances both advection and accumulation of the species. The phenomenon can be represented with a set of nonlinear differential equations that incorporate that feedback and take into account mass-action chemical kinetics, diffusion, advection, and chemical couplings among mineral reactions. Numerical simulations, aided by a linear instability

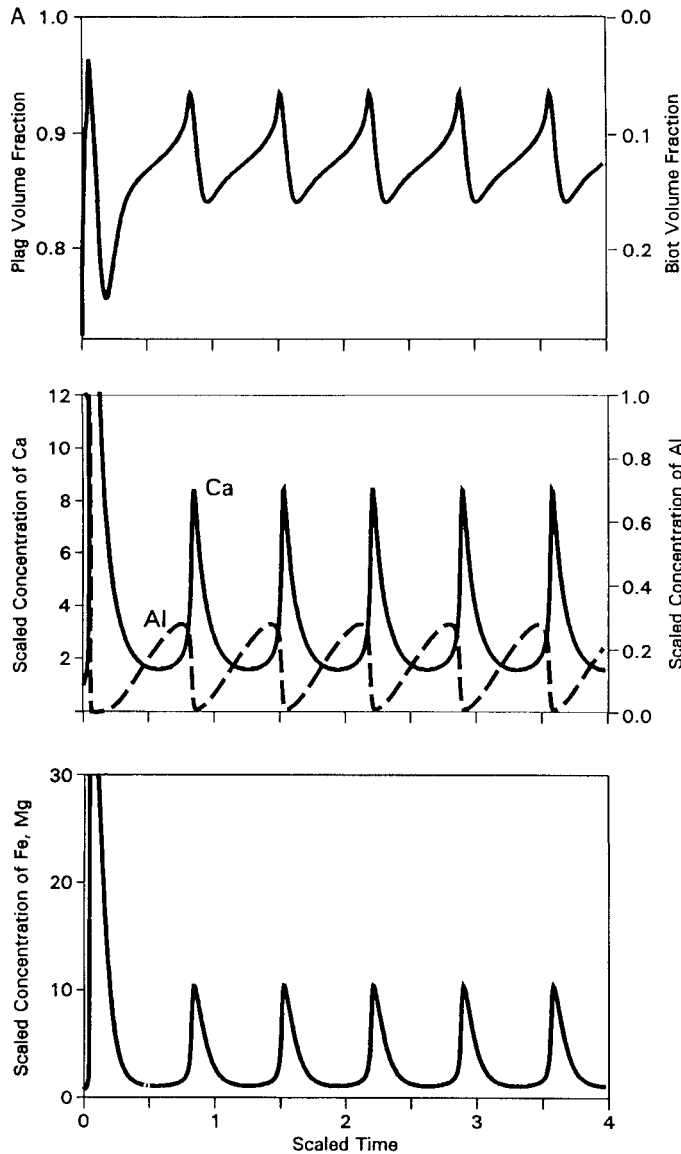


FIG. 4(A).

analysis for the case of crystallization of plagioclase An_{33} by itself, show that the system of equations does have oscillatory solutions under certain conditions. The model produces repetitive layers with thickness that depends on the thickness of the boundary layer, a parameter that could be determined by experiment; it probably lies in the range 0.01–1 cm. The model also is able to predict paired layers (Fig. 5) such as observed in the Stillwater Complex (Boudreau, 1987), although in the simulation shown in Fig. 5 the modal amplitudes are unequal, unlike in the Stillwater doublets. Any desired combination of mode amplitudes and mode wavelength(s) could, we think, be produced by appropriate values of the parameters used, the mineral associations and compositions adopted, and the specific exponents for concentrations adopted in the mass-action rate laws for the minerals involved.

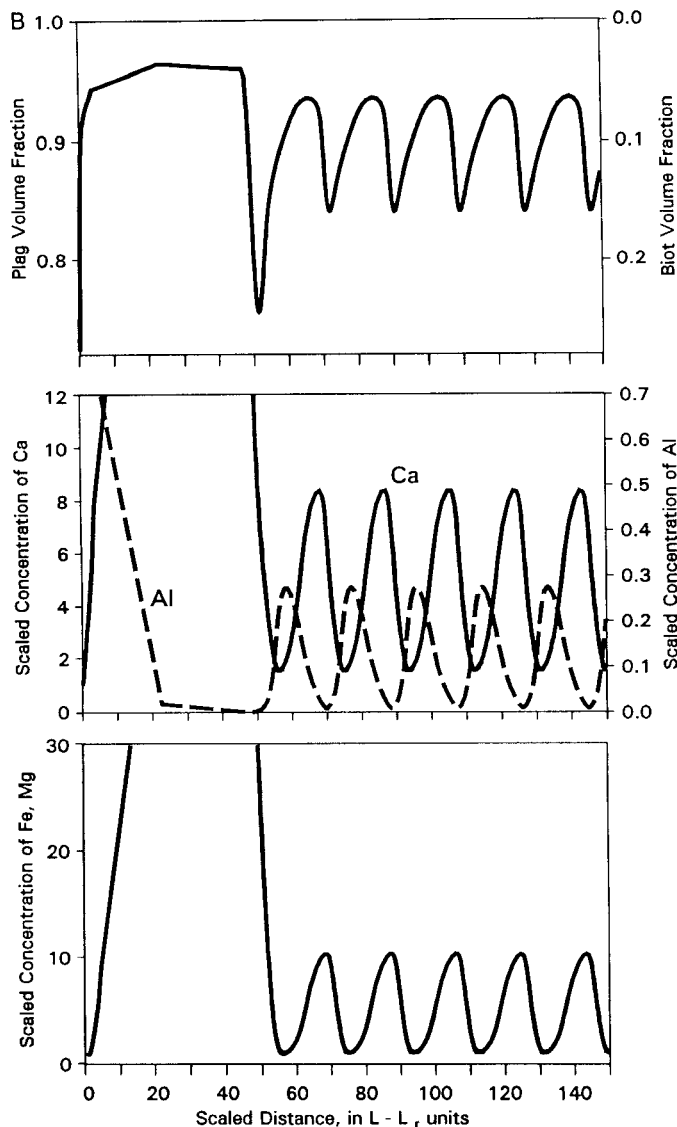


FIG. 4. During crystallization of biotite and plagioclase from a melt, according to the proposed mechanism, the concentrations of melt species in the reaction zone, as well as the produced volume fractions (or modes) of both minerals, oscillate as shown. The curves are obtained by numerical solution of equation (10) using the rate laws $r_{pl} = k_{pl}(Ca^{2+})^3(Al^{3+})$ and $r_{bi} = k_{bi}(Fe^{2+})(Mg^{2+})(Al^{3+})$, and the dimensionless parameter values $\lambda_{pl} = 18.3$, $\lambda_{bi} = 5$, $\theta_{Ca^{2+}} = 0.06$, $\theta_{Fe^{2+}} = 0.1$, $\theta_{Mg^{2+}} = 0.12$, $\theta_{Al^{3+}} = 1$, $\gamma_{Ca^{2+}} = 0.2$, $\gamma_{Fe^{2+}} = 0.05$, $\gamma_{Mg^{2+}} = 0.05$, $\gamma_{Al^{3+}} = 0.494$, $V_{pl}C_{Al^{3+}}^L = 1$, $V_{bi}/V_{pl} = 1.4$. These values are geologically reasonable. (A) Ca^{2+} , Fe^{2+} , Mg^{2+} , and Al^{3+} concentrations in the melt of the reaction zone, and volume fraction of plagioclase and biotite formed, as functions of time. (B) Same data as in (A) but here vs. distance from starting position of the reaction zone. The predicted scale of the layering is the wavelength of one cycle, or about $15(L - L_r)$, where $(L - L_r)$ is the thickness of the boundary layer.

The model suggests that oscillatory crystallization occurs only within very restricted ranges of liquid composition. For example, for the specific (and hypothetical) case of oscillatory crystallization of plagioclase of An_{33} composition, the Al^{3+}/Si^{4+} in the bulk liquid has to be very close to (but less than) $1/2$. This implies that, even if the chemical

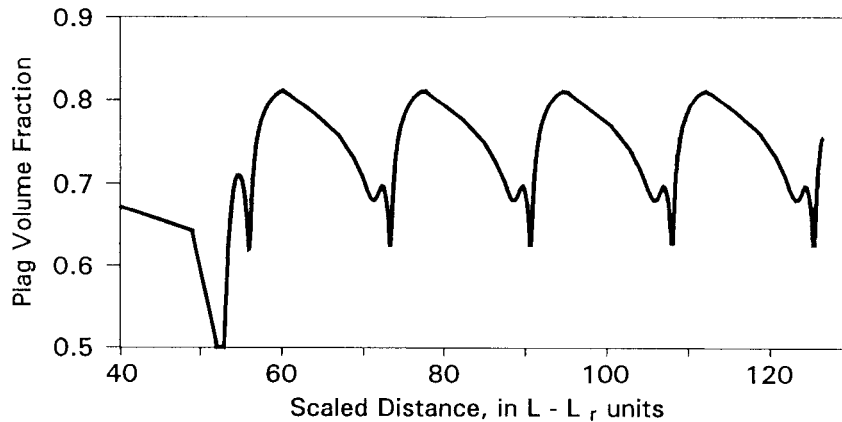


FIG. 5. Numerical simulation producing oscillatory crystallization of biotite and plagioclase in paired layers (or 'doublets'). These doublets do show two different spacings (as in natural examples), but display unequal amplitudes, unlike the Stillwater doublets shown by Boudreau (1987). The plot is obtained as the one in the top frame of Fig. 4B, but using the rate laws $r_{pl} = k_{pl}(Ca^{2+})^3(Al^{3+})^2$ and $r_{bi} = k_{bi}(Fe^{2+})(Mg^{2+})(OH^-)(Al^{3+})$, and the dimensionless parameter values $\lambda_{pl} = 18.3$, $\lambda_{bi} = 5$, $\theta_{Ca^{2+}} = 0.06$, $\theta_{Fe^{2+}} = 0.1$, $\theta_{Mg^{2+}} = 0.12$, $\theta_{OH^-} = 0.1$, $\theta_{Al^{3+}} = 1$, $\gamma_{Ca^{2+}} = 0.3$, $\gamma_{Fe^{2+}} = 0.1$, $\gamma_{Mg^{2+}} = 0.1$, $\gamma_{OH^-} = 0.2$, $\gamma_{Al^{3+}} = 0.493$, $V_{pl}c_{Al^{3+}}^L = 1$, $V_{bi}/V_{pl} = 1.4$.

segregation we invoke is common (and it should be), the occurrence of self-organizational repetitive layering should be restricted, as appears to be the case in nature (e.g., Leveson, 1966; Elliston, 1984; Irvine, 1987b).

Because, according to the model, concentrations of species in the liquid of the reaction zone oscillate, the chemical affinities of the mineral precipitation reactions must also oscillate. These oscillations should cause the rates of nucleation themselves, and thus the crystal sizes produced, to oscillate also. Thus the model can explain some rhythmic layerings in which oscillatory crystal sizes are inconsistent with other mechanisms such as mechanical settling and Ostwald ripening.

Oscillatory crystallization of a silicate liquid by the mechanism proposed here requires that the diffusivity of the accumulated species (Ca^{2+} in the cases of Figs. 3–5; in others, it could be Na^+ and K^+ , or other modifier ions) be larger than that of the depleted species (in our case Al^{3+}). In fact, $D_{Ca^{2+}}$ is indeed greater than $D_{Al^{3+}}$ in silicate melts (e.g., Hess, 1989, p. 67). Species with low charge-to-size ratios are therefore more likely to accumulate in the liquid (upon its crystallization), because they have the higher diffusivities (Chekhmir & Epel'baum, 1991, fig. 11). Thus, the occurrence of oscillatory layering by the mechanism proposed is favored in igneous rocks derived from magmas rich in ions with low charge-to-size ratios such as Na^+ , K^+ , and Ca^{2+} . This prediction coincides with the relatively common occurrence of rhythmic layers in alkaline rocks (e.g., Sørensen, 1969, p. 272; Griffin *et al.*, 1974, p. 21). For magmas rich in Mg^{2+} , which is higher in charge/size ratio, the model predicts only occasional formation of oscillatory layering; this also appears to be true in gabbroic rocks (e.g., McBirney & Noyes, 1979; Boudreau, 1987).

For the proposed feedback to operate, the growth rate of at least one of the layer-forming minerals must depend strongly on the concentration of at least one accumulated chemical species. Because plagioclase is common in igneous layers, we suspect that the exponent of Na^+ or Ca^{2+} concentration must be >1 , perhaps >2 , in the particular version of the rate law [equation (3)] that applies to plagioclase. An experimental test of this prediction would be useful. Numerical simulation shows that when the reaction orders are high enough, equation (10) has oscillatory solutions for various combinations of the exponents in equation

(3), implying that the proposed oscillatory mechanism can work for a wide variety of rate laws.

The mechanism we propose occurs during crystallization through chemical feedbacks between liquid and minerals and among different minerals; these feedbacks work equally well regardless of whether or not the temperature is spatially or temporally uniform. The model does not link the geometry of repetitive layering to that of cooling fronts. It accounts for repetitive layering, but, because it is one-dimensional, it cannot predict the geometry of the layering (spherical, planar, etc.). We suspect that the geometry of igneous self-organizational layerings is probably dictated by the geometry of the initial and boundary conditions in each particular case.

ACKNOWLEDGEMENTS

We thank Abhijit Basu and Kim Sowder of Indiana University, and Bertrand Fritz of the University of Strasbourg, for help. The manuscript was improved thanks to the comments of A. E. Boudreau and H. R. Naslund as reviewers and T. N. Irvine as editor. We are grateful to the U.S. National Science Foundation for support (grants EAR 9003633 and EAR 9104198), the Exchange Program between Nanjing and Indiana Universities for a fellowship, and the Laboratory of Geosciences of the Environment of the University of Marseille for hospitality during our sabbatical.

REFERENCES

- Allègre, C. J., Provost, A., & Jaupart, C., 1981. Oscillatory zoning: a pathological case of crystal growth. *Nature* **294**, 223–8.
- Baronnet, A., 1982. Ostwald ripening in solution. The case of calcite and mica. *Estudios Geol.* **38**, 185–98.
- Berner, R. A., 1980. *Early Diagenesis: A Theoretical Approach*. Princeton, NJ: Princeton University Press, 241 pp.
- Boudreau, A. E., 1987. Pattern formation during crystallization and the formation of fine-scale layering. In: Parsons, I. (ed.) *Origins of Igneous Layering*. Boston, MA: Reidel, 453–71.
- Brandeis, G., Jaupart, C., & Allègre, C. J., 1984. Nucleation, crystal growth and the thermal regime of cooling magmas. *J. Geophys. Res.* **89**(B12), 10 161–77.
- Campbell, I. H., 1978. Some problems with the cumulus theory. *Lithos* **11**, 311–23.
- Chekhmir, A. S., & Epel'baum, M. B., 1991. Diffusion in magmatic melts: new study. In: Perchuk, L. L. & Kushiro, I. (eds.) *Physical Chemistry of Magmas*. Berlin: Springer-Verlag, 99–119.
- Cook, P. A., 1986. *Nonlinear Dynamical Systems*. Englewood Cliffs, NJ: Prentice-Hall, 216 pp.
- Elliston, J. N., 1984. Orbicules: an indication of the crystallization of hydrosilicates, I. *Earth-Sci. Rev.* **20**, 265–334.
- Emeleus, C. H., 1963. Structural and petrographic observations on layered granites from southern Greenland. *Miner. Soc. Am. Special Paper* **1**, 22–9.
- Ghiorso, M. S., 1987. Chemical mass transfer in magmatic processes III. Crystal growth, chemical diffusion and thermal diffusion in multicomponent silicate melts. *Contr. Miner. Petrol.* **96**, 291–313.
- Griffin, W. L., Heier, K. S., Taylor, P. N., & Weigand, P. W., 1974. General geology, age and chemistry of the Raftund mangerite intrusion, Lofoten–Vestralen. *Norges Geol. Undersøkelse* **312**, 1–30.
- Hess, P. C., 1989. *Origins of Igneous Rocks*. Cambridge, MA: Harvard University Press, 336 pp.
- Irvine, T. N., 1987a. Layering and related structures in the Duke Island and Skaergaard intrusions: similarities, differences, and origins. In: Parsons, I. (ed.) *Origins of Igneous Layering*. Boston, MA: Reidel, 185–245.
- 1987b. Processes involved in the formation and development of layered igneous rocks. *Ibid.*, 649–56.
- Jahns, R. H., & Tuttle, O. F., 1963. Layered pegmatite–aplite intrusives. *Miner. Soc. Am. Special Paper* **1**, 78–92.
- Kirkpatrick, R. J., 1976. Towards a kinetic model for the crystallization of magma bodies. *J. Geophys. Res.* **81**(14), 2565–71.
- Leveson, D. J., 1963. Orbicular rocks of the Lonesome Mountain area, Beartooth Mountains, Montana and Wyoming. *Geol. Soc. Am. Bull.* **74**, 1015–40.
- 1966. Orbicular rocks: a review. *Ibid.* **77**, 409–26.
- Maaløe, S., 1987. Rhythmic layering of the Skaergaard intrusion. In: Parsons, I. (ed.) *Origins of Igneous Layering*. Boston, MA: Reidel, 247–62.
- McBirney, A. R., & Noyes, R. M., 1979. Crystallization and layering of Skaergaard intrusion. *J. Petrology* **20**, 487–554.
- White, C. M., & Boudreau, A. E., 1990. Spontaneous development of concentric layering in a solidified siliceous dike, East Greenland. *Earth-Sci. Rev.* **29**, 321–30.

- Morse, J. W., & Casey, W. H., 1988. Ostwald processes and mineral paragenesis in sediments. *Am. J. Sci.* **288**, 537–60.
- Nabelek, P. I., Taylor, L. A., & Lofgren, G. E., 1978. Nucleation and growth of plagioclase and the development of textures in a high-alumina basaltic melt. *Proc. Lunar Planet. Sci. Conf. 9th*, 725–41.
- Naslund, H. R., Turner, P. A., & Keith, D. W., 1991. Crystallization and layer formation in the middle zone of the Skaergaard intrusion. *Bull. Geol. Soc. Denmark* **38**, 165–71.
- Nicolis, G., & Prigogine, I., 1977. *Self-Organization in Non-Equilibrium Systems*. New York: John Wiley, 491 pp.
- Parsons, I., 1987. *Origins of Igneous Layering*. Boston, MA: Reidel, 666 pp.
- Samoylovich, Y. A., 1979. Oscillatory crystallization of a magma. *Geochem. Int.* **16**(3), 79–84.
- Sørensen, H., 1969. Rhythmic igneous layering in peralkaline intrusions. *Lithos* **2**, 261–83.
- Verhoogen, J., Turner, F. J., Weiss, L. E., Fyfe, W. S., & Wahrhaftig, C., 1970. *The Earth*. New York: Holt, Rinehart and Winston, 748 pp.
- Wager, L. R., & Brown, G. M., 1968. *Layered Igneous Rocks*. Edinburgh: Oliver & Boyd, 588 pp.
- Wang, Y., & Merino, E., 1990. Self-organizational origin of agates: banding, fiber twisting, composition, and dynamic crystallization model. *Geochim. Cosmochim. Acta* **54**, 1627–38.
- . 1992. Dynamic model of oscillatory zoning of trace elements in calcite: double layer, inhibition and self-organization. *Ibid.* **56**, 587–96.

APPENDIX

Before the linear instability analysis and numerical simulation for a specific system, we scale equation (10), with the parameters in the equation being reduced to fewer independent dimensionless ones. The dimensionless parameters for the cases of growth of only An_{33} plagioclase and plagioclase/biotite are defined as follows:

$$\eta = \frac{[8 - (c_s/c_{Ca^{2+}}^L)]D_{Al^{3+}}}{[8 - 4(c_s/c_{Al^{3+}}^L)]D_{Ca^{2+}}}$$

$$\theta_j = D_{Al^{3+}}/D_j$$

$$\gamma_j = c_j^L/c_s$$

$$\lambda_i = \frac{(L - L_r)^2 \beta}{D_{Al^{3+}} c_{Al^{3+}}^L} k_i \prod_j (c_j^L)^{a_{ij}}$$

where c_j^L is the concentration of species j outside the boundary layer.